RSC Advances

PAPER

View Article Online
View Journal | View Issue

Cite this: *RSC Adv.*, 2016, **6**, 43429

Ni/Al_2O_3/epoxy high-*k* composites with ultralow nickel content towards high-performance dielectric applications

Jing Wang,[a] Zhicheng Shi,*[a] Fan Mao,[a] Xin Wang,[a] Kun Zhang[b] and Jing Shi*[a]

Received 8th March 2016
Accepted 26th April 2016

DOI: 10.1039/c6ra06157e

www.rsc.org/advances

Nickel/alumina/epoxy three-phase composites consisting of nickel particles dispersed in alumina/epoxy composite matrix were prepared using a facile wet impregnation process. The influences of *in situ* formed alumina particles (i-Al_2O_3) and epoxy on the dielectric properties of the composites were investigated in detail. For the composites with nickel contents far below the percolation threshold, the main electrical conduction mechanism is hopping conduction, and the main loss comes from polarizations. Therefore, the formation of alumina and epoxy result in higher permittivity but high loss due to the enhanced interfacial polarization. For the composites with nickel contents below but near the percolation threshold, the main electrical conduction mechanism is metal-like conduction and the main loss comes from eddy currents under high frequency electric field. Accordingly, the i-Al_2O_3 and filled epoxy between nickel particles could bring both high permittivity and low loss. This paper experimentally shows how the characteristics of the interface between different phases influence the dielectric performances of composites. And the impregnation process is an effective strategy to obtain percolative metal/ceramic/polymer three-phase composites with ultralow metal content, high permittivity and low loss.

Introduction

High-performance dielectric materials with high permittivity (high-*k*) and low loss have wide applications in microstrip antennas,[1] high-density energy storage,[2–4] electrical stress control and actuators, *etc.*[5–7] In order to achieve high permittivity, ferroelectrics could be a good choice. However, the intrinsic high dielectric loss and low dielectric strength of ferroelectrics are still great challenges. That is to say, it is difficult to realize simultaneous high permittivity, low loss and high dielectric strength in single phase materials. As an alternative, composite materials may be promising candidates for high-*k* applications. As we know, the dielectric properties of a composite will undergo significant changes near its percolation threshold,[8–11] and numerous researches have confirmed that percolative composites are promising candidates for high-*k* materials with outstanding dielectric properties, such as tunable high permittivity, high dielectric strength, low loss, *etc.* Therefore, various strategies have been developed to obtain high-*k* according to percolation theory in composite materials, such as ferroelectric/polymer composites,[12–14] binary or ternary metal (or carbon)/polymer composites,[15–17] metal (or carbon)/ceramic composites, *etc.*[18–21] In these composites, a certain volume fraction (lower than but still near the percolation threshold) of metal, carbon or ferroelectric powders should be dispersed into the matrix to achieve excellent dielectric performance. However, the percolation thresholds of the composites are usually high, leading to high leakage conductance loss, eddy current loss and dielectric loss. Inui *et al.*[1] experimentally confirmed that, for $BiTiO_3$/cellulose nanopaper composites consisting of $BiTiO_3$ particles dispersed in cellulose nanopaper, the permittivity can only be enhanced from 5.3 to 8.1 even if the volume fraction of the ferroelectric fillers is as high as 20.9 vol%. Therefore, silver nanowires were adopted as the fillers to achieve high permittivity and low percolation threshold in their work. However, the agglomeration of the nano-scale fillers may result in severe consequences, such as significantly enhanced leakage conductance loss, unstable dielectric performances, deteriorated dielectric strength and mechanical properties, *etc.* As discussed above, the realization of low percolation threshold and homogeneous distribution of fillers are the two main problems that hinder the percolative composites from being promising candidates for high performance dielectric applications. Therefore, huge efforts have been paid to the preparation of percolative composites with ultralow percolation threshold and homogeneously dispersed fillers. To lower the percolation threshold of the composite, fillers with high aspect ratio, such as metal nanowires, carbon nanotubes and carbon nanofibers, are usually chosen.[22–26] However, how to

[a]*Institute of Materials Science and Engineering, Ocean University of China, Qingdao 266100, P. R. China. E-mail: zcshi@ouc.edu.cn; shijing@ouc.edu.cn*

[b]*Key Laboratory of Microgravity (National Microgravity Laboratory), Institute of Mechanics, Chinese Academy of Sciences, 15 Beisihuanxi Road, Beijing 100190, China*

realize the homogeneous distribution of these nano-scale fillers in the matrix turns to be a great challenge. Up to now, many methods have been proposed, among which the surface modification process has been proved to be an effective way to prepare homogeneous percolative high-*k* composites with improved dielectric strength and dielectric loss.[27–31]

Although numerous binary or ternary percolative high-*k* composites consisting of various surface modified fillers have been proposed in recent years, the preparation of high-*k* composites with ultralow percolation threshold, homogeneously distributed fillers and low loss is still found to be difficult. In our previous work, a facile wet chemical process was proposed to obtain porous metal/ceramic composites with ultralow percolation threshold and significantly enhanced permittivity. In those porous metal/ceramic composites, metal particles dispersed on the pore walls of porous ceramic, leading to the ultralow percolation threshold, hence the suppressed leakage conductance loss and eddy current loss.[10,11,32] Similarly, Ameli *et al.*[33] prepared a class of porous polymer nanocomposites consisting of multi-walled carbon nanotubes (MWCNT) dispersed on the pore walls of porous polymer. And it is shown that the porous MWCNT/polymer composites exhibit significantly high permittivity, ultralow percolation threshold and low dielectric loss. That is to say, the porous conductor/insulator composites have great potential for high performance dielectric applications. As discussed above, porous conductor/insulator composites could be good candidates for high-*k* materials. However, the porous microstructure will result in the decrease of permittivity because of the low dielectric constant of air. Moreover, the leakage conductance and eddy current loss at high frequency is high due to the fact that the breakdown strength of air is much lower than insulating ceramics or polymers. That is to say, the pores should be filled with insulating materials, and epoxy is a good candidate due to its excellent dielectric property.

In this paper, a class of porous nickel/alumina composites with ultralow nickel content are prepared *via* a wet chemical process described in our previous work.[32] Moreover, the $Al(NO_3)_3$ is added into impregnation solution as the precursor of *in situ* formed alumina (i-Al_2O_3), which could separate the nickel particles from each other. In order to improve the dielectric property of composites, epoxy is further filled into the pores to form Ni/Al_2O_3/epoxy three phase composites.

Results and discussion

The X-ray diffraction (XRD) patterns of the Ni/Al_2O_3 composites using $Ni(NO_3)_2$ solution (solution A: 1 mol L^{-1} Ni^{2+}) and $Ni(NO_3)_2$/$Al(NO_3)_3$ solution (solution B: 1 mol L^{-1} Ni^{2+} + 0.5 mol L^{-1} Al^{3+}) are shown in Fig. 1. As shown in Fig. 1a–c, the Ni/Al_2O_3(A) composites (prepared by solution A) are composed of nickel and alumina, no other additional phases are observed. As shown in Fig. 1d–f, the components of Ni/Al_2O_3(B) composites (prepared by solution B) are nickel and alumina, where the alumina consists of alumina matrix and *in situ* formed alumina (i-Al_2O_3). There are no differences in components between the composites prepared by two kinds of impregnation solutions. It

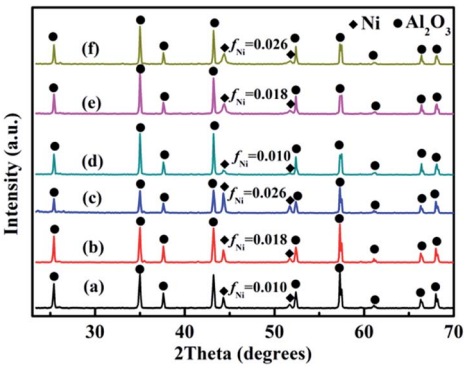

Fig. 1 XRD patterns of the composites with different nickel contents prepared using solution A (a–c) and solution B (d–f).

indicated that there is no existence of $Al(NO_3)_3$ after calcination and reduction, and the crystal structure of i-Al_2O_3 is same as alumina matrix. Furthermore, the addition of $Al(NO_3)_3$ has no influence on the transformation of $Ni(NO_3)_2$ into Ni, and nickel oxides were totally reduced into nickel during the reduction process. As we know, high temperature (>1000 °C) may result in the reactions between nickel and alumina,[34–36] leading to the appearance of unexpected phases in the composites. In the present work, the Ni/Al_2O_3 composites were prepared *via* a low temperature impregnation–reduction process. Accordingly, harmful reactions between nickel and alumina could be avoided.

Fig. 2 shows the fractured surface scanning electron microscope (SEM) images of the composites prepared using solution A. As shown in Fig. 2a–c, nickel particles are homogeneously distributed on the pore walls of porous alumina matrix in the

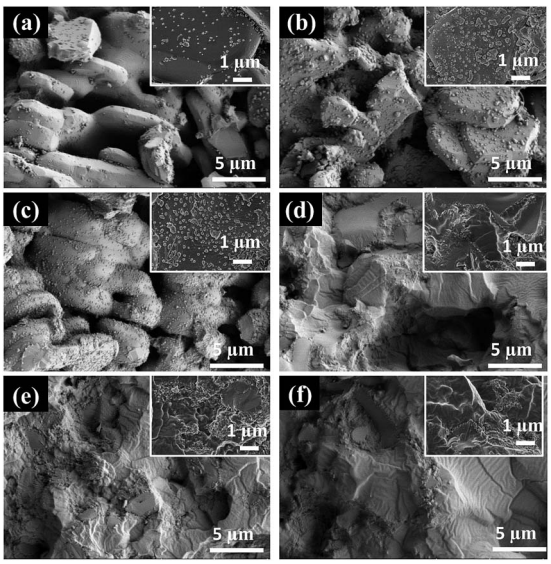

Fig. 2 SEM images of Ni/Al_2O_3(A) and Ni/Al_2O_3/EP(A) composites; (a–c) are the Ni/Al_2O_3(A) composites with nickel contents of 1.0 vol%, 1.8 vol% and 2.6 vol%, respectively; (d–f) are the Ni/Al_2O_3/EP(A) composites with nickel contents of 1.0 vol%, 1.8 vol% and 2.6 vol%, respectively.

Ni/Al_2O_3(A) composites. And the distance between nickel particles become closer with increasing nickel content. When the nickel content reaches 2.60 vol%, some nickel particles interconnect with each other, leading to the appearance of localized nickel networks (Fig. 2c). Then, the iron/alumina interface area will be significantly enlarged due to the formation of localized nickel networks, and the composites can be regarded as a supercapacitor consisting of numerous "micro-capacitors". As we know, when the nickel content reaches the percolation threshold, three dimensional nickel networks will be formed throughout the composite. And the percolative composites with high metal content could manifest very high dielectric permittivity due to the sharply increased amount of equivalent "micro-capacitors". Furthermore, when the nickel content exceeds the percolation threshold, negative permittivity behavior will appear, which is very attractive for double negative metamaterials.[10,11,37–40] However, the severe leakage conductance phenomenon and high loss are still challenges for meta-composites with negative permittivity.[8,10] As discussed above, in order to obtain high-k and low loss, the nickel contents should be near but lower than the percolation threshold. In the present work, the majority of the nickel particles are still isolated as shown in Fig. 2a–c. As shown in Fig. 2d–f, the pores of Ni/Al_2O_3(A) composites can be well filled with epoxy *via* the impregnation–solidification process. The XRD and SEM results indicate that the impregnation process is an effective way to prepare Ni/Al_2O_3/EP composites with homogeneous microstructures. Our recent researches show that, the morphology of nickel in the composites can be well adjusted by the impregnation conditions and hydrothermal treatment. And various nickel nanostructures, such as wires, stacked disks, porous particles, can be *in situ* formed on the pore walls of the porous alumina. And these unique metallic nanostructures could effectively lower the percolation threshold of composites and increase the interface area of nickel/alumina and nickel/epoxy, which are very beneficial for the reduced dielectric loss and enhanced dielectric permittivity.

Fig. 3 shows the frequency dispersions of σ_{ac} for composites with different nickel loadings. We can see that, the σ_{ac} increases with increasing nickel content for both of the Ni/Al_2O_3 and Ni/Al_2O_3/EP composites. However, the dependences of σ_{ac} are different for the composites with different nickel contents. As shown in Fig. 3a, the ac conductivities σ_{ac} of the Ni/Al_2O_3(A) composites with nickel contents of 1.0 vol% and 1.8 vol% increase with frequency, and the σ_{ac}–ω relationships of the composites follow the power law $\sigma_{ac} \propto \omega_n$ $(0 < n < 1)$, indicating the hopping conduction behaviour.[24] When the nickel content reaches 2.6 vol%, the σ_{ac} decreases slowly with increasing frequency. As mentioned above, localized nickel networks are formed in the Ni/Al_2O_3(A) composites with nickel content of 2.6 vol% (Fig. 2c). That is to say, 2.6 vol% is near the percolation threshold. Therefore, the Ni/Al_2O_3 ($f_{Ni} = 0.026$) composite shows the metal-like frequency dispersion of conductivity due to the overwhelming contribution of skin effect relative to hopping conduction behaviour at high frequencies. As is known to us, σ_{ac} decreases with decreasing skin depth. And the skin depth of lossy media can be expressed as $\delta = (2/\sigma\omega\mu_r)^{1/2}$, where

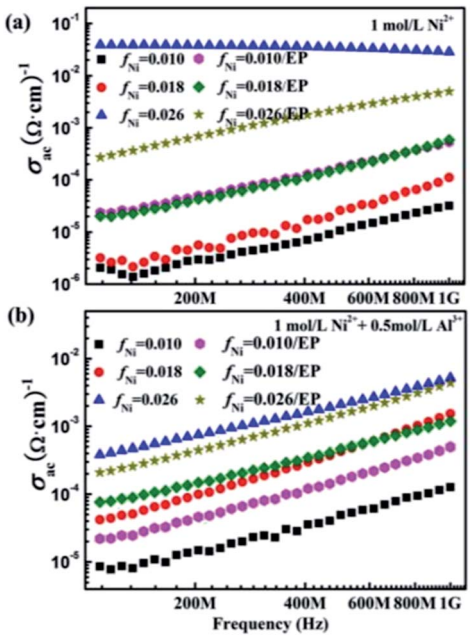

Fig. 3 Frequency dispersions of ac conductivity for the Ni/Al_2O_3(A) and Ni/Al_2O_3/EP(A) composites (a), Ni/Al_2O_3(B) and Ni/Al_2O_3/EP(B) composites (b).

δ is the skin depth, σ is the DC conductivity, ω is the frequency ($\omega = 2\pi f$), and μ_r is the relative permeability. Generally, σ is constant for a certain material. Meanwhile, the value of μ_r could also be regarded as a constant ($\mu \approx 1.0$) at high frequency due to the fact that the cut-off frequency of a magnetic material is usually below 1 GHz. Consequently, the skin depth decreases with higher frequency, leading to the decrease of ac conductivity σ_{ac}.

Comparing the σ_{ac} of Ni/Al_2O_3(A) and Ni/Al_2O_3/EP(A) composites shown in Fig. 3a, it is indicated that the filling of epoxy is not an effective way to reduce the conductivity for the composites with low nickel contents (1.0 vol% and 1.8 vol%). Nevertheless, when the nickel content is 2.6 vol%, the filling of epoxy can effectively reduce the σ_{ac} of the composite. For the composites with low nickel contents, the distance between nickel particles is large and it is difficult to form conductive pathways under the tested ac electric field. In other words, the composites with nickel contents of 1.0 vol% and 1.8 vol% are equivalent to capacitors. Therefore, the formation of epoxy layer between nickel particles will result in the increased capacitance of the equivalent capacitors, leading to the slight increase of ac conductivity rather than suppressed conductivity. When the nickel content is high, the distance between nickel particles is small enough to form conductive pathways under the tested ac electric field, and the composite is equivalent to an inductor which manifests metal-like conduction behaviour. Accordingly, the epoxy layers between nickel particles are equivalent to resistors which could effectively reduce the conductivity. Similarly, the function of the *in situ* formed alumina particles ($i\text{-}Al_2O_3$) is the same as the epoxy layers between nickel particles. Therefore, the values of σ_{ac} and frequency dispersion characteristics of the composites prepared using $Ni(NO_3)_2$ and

$Ni(NO_3)_2/Al(NO_3)_3$ solutions are similar when the nickel contents are 1.0 vol% and 1.8 vol% (Fig. 3a and b). And when the nickel content reaches 2.6 vol%, the σ_{ac} of the composites prepared using $Ni(NO_3)_2$ solution is much higher than the composites prepared using $Ni(NO_3)_2/Al(NO_3)_3$ solutions. Moreover, the σ_{ac} of the composites $f_{Ni} = 0.026$/EP (1 mol L^{-1} Ni^{2+}, Fig. 3a) and $f_{Ni} = 0.026$/EP (1 mol L^{-1} Ni^{2+} + 0.5 mol L^{-1} Al^{3+}, Fig. 3b) are similar to each other because of the similar influences of epoxy and i-Al_2O_3 on the composites' conduction behaviours. Based on the above discussions, we can conclude that the distribution of nickel particles in the composites is tunable with composition of the impregnation solution, leading to different frequency dispersion behaviours of conductivity. Although the *in situ* formation of insulating layers (i-Al_2O_3 or epoxy) between nickel particles is not an effective way to reduce the high frequency ac conductivity for the composites with nickel contents far below the percolation threshold, it is an effective method for percolative composites with nickel content near the percolation threshold.

The dielectric spectra of the composites prepared using solution A are shown in Fig. 4. We can see that, the real part of permittivity ε' increases with higher nickel content due to the increase of the interface area between nickel, alumina and epoxy (Fig. 4a). Furthermore, a significant enhancement of ε' is observed when the nickel content increases from 1.8 vol% to 2.6 vol% for the Ni/Al_2O_3/EP(A) composites, this phenomenon could attribute to the Maxwell–Wagner–Sillars effect near percolation threshold. However, the Ni/Al_2O_3(A) with nickel content of 2.6 vol% ($f_{Ni} = 0.026$ in Fig. 4a) shows a remarkable different frequency dispersion behaviour compared with the other composites. Correspondingly, the $f_{Ni} = 0.026$ composite exhibits a significant dielectric loss as high as tan $\delta \approx 100$ at low frequency (Fig. 4b). Similar dielectric dispersion behaviours and high dielectric loss have been observed in other conductor/insulator composites near the percolation threshold due to the overwhelming leakage conductance phenomenon.[41,42] Generally speaking, the significant differences in conductivity between nickel (10^5 Ω^{-1} cm^{-1}) and alumina (10^{-13} Ω^{-1} cm^{-1}) could result in the accumulation of charges on the nickel–alumina interfaces. When the composite is put into an external alternating electric field, the interfacial polarization phenomenon occurs. At low frequencies, the interfacial polarization could keep up with the change of external alternating electric field, and the charge accumulation leads to the enhancement of real permittivity ε'. However, the interfacial polarization will gradually lag behind the external electric field with increasing frequency, leading to the decrease of ε'. However, when the nickel content is near or above the percolation threshold, the composites dielectric spectra will follow the Drude model,[10,11,41,42] leading to the anomalous frequency dispersion of permittivity (Fig. 4a). Comparing the dielectric spectra of Ni/Al_2O_3(A) and Ni/Al_2O_3/EP(A) composites in Fig. 4a, a distinct enhancement of permittivity can be observed because of the filling of epoxy, and that should be attributed to the enlarged interface areas between epoxy and Ni/Al_2O_3(A) composite. This is due to the fact that the composite can be regarded as a supercapacitor consisting of numerous "micro-capacitors". The filling of insulating epoxy can increase the amount of "micro-capacitors", leading to the enhancement of permittivity. Especially, the Ni/Al_2O_3/EP(A) composite with nickel content of 2.6 vol% shows a much higher permittivity and lower loss ($\varepsilon'_r \approx 65$, tan $\delta \approx 0.1$ at 100 MHz) compared with the Ni/Al_2O_3(A) composite ($f_{Ni} = 0.026$, $\varepsilon'_r \approx 18$, tan $\delta \approx 80$ at 100 MHz). Nevertheless, the losses of $f_{Ni} = 0.010$/EP and $f_{Ni} = 0.018$/EP are higher than those of $f_{Ni} = 0.010$ and $f_{Ni} = 0.018$ (Fig. 4b). For the composites far below the percolation threshold (1.0 vol% and 1.8 vol% nickel), the main loss comes from dielectric polarization. While for the composite near the percolation threshold (2.6 vol% nickel), the main loss comes from the leakage conductance and eddy current. Consequently, the formation of epoxy layer between nickel particles could reduce the loss of the percolative nickel/alumina composite near the percolation threshold due to the suppressed leakage conductance loss. Meanwhile, the epoxy layer in the composites far below the percolation threshold will increase the composites' losses due to the enhanced interfacial polarization processes taken place on the Ni–epoxy and Al_2O_3–epoxy interfaces.

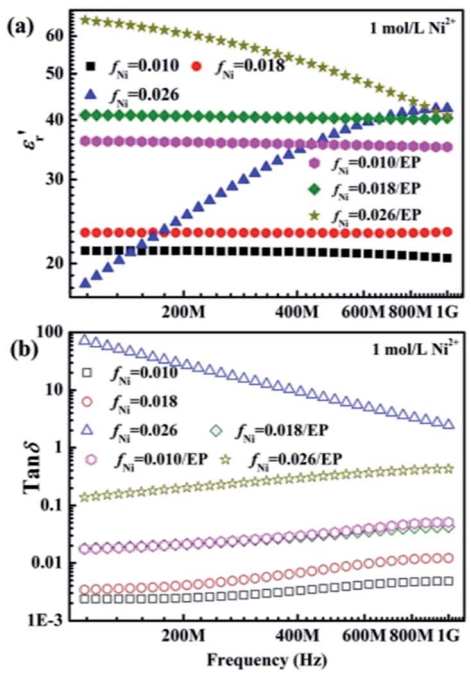

Fig. 4 Frequency dispersions of real permittivity (a) and loss (b) for the Ni/Al_2O_3(A) and Ni/Al_2O_3/EP(A) composites.

Fig. 5 shows the dielectric spectra of the Ni/Al_2O_3(B) and Ni/Al_2O_3/EP(B) composites. Similar to the composites prepared using solution A, higher nickel content and the filling of epoxy result in the increase of real dielectric permittivity (Fig. 5a). Moreover, the filling of epoxy also leads to the increase of tan δ for the composites with nickel contents of 1.0 vol% and 1.8 vol%, and the decrease of tan δ for the composite with nickel content of 2.6 vol%. Comparing Fig. 4a and 5a, we can see that the *in situ* formation of alumina between nickel particles can enhance the dielectric permittivity due to the enlarged Ni–Al_2O_3 and epoxy–Al_2O_3 interface areas. As shown in Fig. 4b and 5b, for

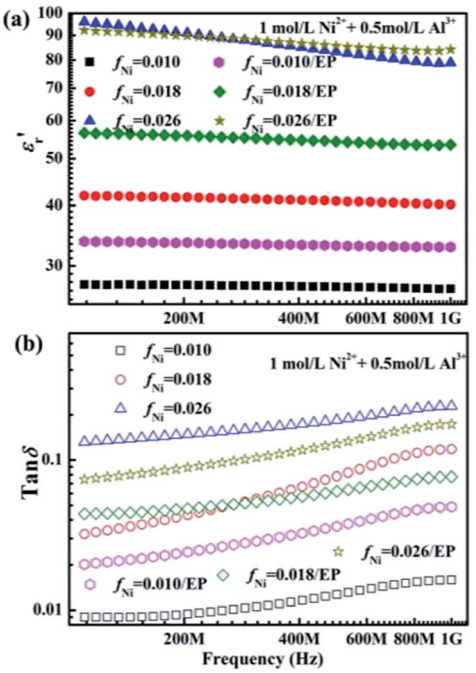

Fig. 5 Frequency dispersion of real permittivity (a) and loss (b) for the Ni/Al_2O_3(B) and Ni/Al_2O_3/EP(B) composites.

the composites with nickel content of 1.0 vol% and 1.8 vol%, the i-Al_2O_3 bring in higher loss; for the composite with nickel content of 2.6 vol%, the i-Al_2O_3 could suppress the loss. When $Al(NO_3)_3$ added into the solution, Ni particles would be covered by i-Al_2O_3 particles after calcination. The existence of i-Al_2O_3 between Ni particles makes them isolated from each other. That is to say, the i-Al_2O_3 and epoxy play similar roles with regard to the dielectric performance of Ni/Al_2O_3/EP composites. Similarly, the enhancement of permittivity and the suppression of loss were also observed in other composites containing *in situ* formed insulating layers between conductive fillers.[43–45]

Experimental

Preparation of the composites

The preparation of Ni/Al_2O_3/EP composites is as follows: (1) two kinds of impregnation solutions (A and B) consisting of $Ni(NO_3)_2$ and $Al(NO_3)_3$ (purity ≥ 99.8%, purchased from Sinopharm Chemical Reagent Co., Ltd.) dissolved in ethanol were prepared. In solution A, the concentration of Ni^{2+} is 1.0 mol L^{-1}, without Al^{3+} addition; in solution B, the concentration of Ni^{2+} and Al^{3+} are 1.0 mol L^{-1} and 0.5 mol L^{-1}, respectively. Then, the porous alumina (Al_2O_3) discs with open porosity of 50% were soaked and vacuumized for 10 min in the impregnation solution. After the excess solution on the surface rubbed off, the discs were embedded into Al_2O_3 powders, and dried at 343 K for 2 h and 373 K for 2 h to remove ethanol. (2) The discs were calcined at 623 K in the air for 20 min to obtain the NiO and i-Al_2O_3 (*in situ* formed alumina) precursors ($2Ni(NO_3)_2 = 2NiO + 4NO_2\uparrow + O_2\uparrow$, $4Al(NO_3)_3 = 2Al_2O_3 + 12NO_2\uparrow + 3O_2\uparrow$). Then the NiO precursors were reduced at 873 K under the reduction atmosphere (10% H_2/90% Ar) for 3 h to get Ni/Al_2O_3 composites. The composites with Ni content of 1.0 vol%, 1.8 vol% and 2.6 vol% were prepared. (3) The Ni/Al_2O_3 composites were soaked in epoxy/polyimide mixture ($V_{epoxy}/V_{polyimide} = 1:1$, the polyimide as curing agent of epoxy) at 373 K and vacuumized for 10 min to "press" the mixture into the porous matrix. Then, the discs were taken out and the excess mixture on the surface was rubbed off. After the solidification at 373 K for 2 h, Ni/Al_2O_3/EP three-phase composites were prepared.

Characterization

The fracture surface morphologies of the composites were obtained by SU-8020 Field Emission Scanning Electron Microscope. X-ray diffraction (XRD) patterns were recorded in air and at room temperature using the Rigaku D/max-rB X-ray diffractometer with CuKα radiation. For the permittivity measurements, the discs with silver electrodes were put between the two planar electrodes of 16453A dielectric test fixture for permittivity measurements. The permittivity measurements were carried out under AC voltage 100 mV at room temperature from 10 MHz to 1 GHz using Agilent E4991A Impedance Analyzer.[46] The conductivity σ is calculated using real and imaginary permittivity ($\sigma = 2\pi f\varepsilon''_r\varepsilon_0$).

Conclusions

We experimentally investigated the influence of *in situ* formed alumina and filled epoxy on the dielectric properties of the nickel/alumina composites with ultralow nickel content in this paper. It is demonstrated that for the composites with nickel content far below the percolation threshold, the *in situ* formed alumina and filled epoxy result in enhanced permittivity and higher loss; for the composites with nickel contents below but near the percolation threshold, the alumina and epoxy between nickel particles could bring simultaneous enhanced permittivity and lower loss. That is to say, the modified impregnation process is an effective strategy to obtain high performance high-*k* metal/ceramic/polymer three-phase composites with ultralow metal content. And the clarification of the relationship between the composite's microstructures and its dielectric performances will have great significance for the development of dielectric functional materials.

Acknowledgements

This work was supported by the National Natural Science Foundation of China (51402271, 51401028), Foundation for Outstanding Young Scientist in Shandong Province (BS2014CL003), Project Funded by China Postdoctoral Science Foundation (2014M550375, 2015T80748), Qingdao Science and Technology Plan (14-2-4-118-jch), Fundamental Research Funds for the Central Universities (201413001), Projects Funded by Shandong and Qingdao Postdoctoral Science Foundation.

Notes and references

1 T. Inui, H. Koga, M. Nogi, N. Komoda and K. Suganuma, A Miniaturized Flexible Antenna Printed on a High Dielectric

Constant Nanopaper Composite, *Adv. Mater.*, 2015, **27**, 1112–1116.

2 Y. Yang, H. L. Sun, D. Yin, Z. H. Lu, J. H. Wei, R. Xiong, J. Shi, Z. Y. Wang, Z. Y. Liu and Q. Q. Lei, High Performance of Polyimide/$CaCu_3Ti_4O_{12}$@Ag Hybrid Films with Enhanced Dielectric Permittivity and Low Dielectric Loss, *J. Mater. Chem. A*, 2015, **3**, 4916–4921.

3 M. S. Islam, Y. L. Qiao, C. B. Tang and H. J. Ploehn, Terthiophene-Containing Copolymers and Homopolymer Blends as High-Performance Dielectric Materials, *ACS Appl. Mater. Interfaces*, 2015, **7**, 1967–1977.

4 X. Y. Huang and P. K. Jiang, Core-Shell Structured High-*k* Polymer Nanocomposites for Energy Storage and Dielectric Applications, *Adv. Mater.*, 2015, **27**, 546–554.

5 Q. M. Zhang, H. Li, M. Poh, H. Xu, Z. Y. Cheng and F. Xia, An All-Organic Composite Actuator Material with a High Dielectric Constant, *Nature*, 2002, **419**, 284–287.

6 Z. M. Dang, J. K. Yuan, J. W. Zha, T. Zhou, S. T. Li and G. H. Hu, Fundamentals, Processes and Applications of High-permittivity Polymer–matrix Composites, *Prog. Mater. Sci.*, 2012, **57**, 660–723.

7 Z. M. Dang, J. K. Yuan, S. H. Yao and R. J. Liao, Flexible Nanodielectric Materials with High Permittivity for Power Energy Storage, *Adv. Mater.*, 2013, **25**, 6334–6365.

8 G. Li, S. H. Yu, R. Sun and D. Lu, Clean and *in situ* synthesis of copper–epoxy nanocomposite as a matrix for dielectric composites with improved dielectric performance, *Compos. Sci. Technol.*, 2015, **11**, 95–102.

9 X. Zhang, Y. Shen, Q. H. Zhang, L. Gu, Y. H. Hu, J. W. Du, Y. H. Lin and C. W. Nan, Ultrahigh Energy Density of Polymer Nano Composites Containing $BaTiO_3$@TiO_2 Nanofibers by Atomic-Scale Interface Engineering, *Adv. Mater.*, 2015, **27**, 819–824.

10 Z. C. Shi, R. H. Fan, Z. D. Zhang, L. Qian, M. Gao, M. Zhang, L. T. Zheng, X. H. Zhang and L. W. Yin, Random composites of nickel networks supported by porous alumina toward double negative materials, *Adv. Mater.*, 2012, **24**, 2349–2352.

11 Z. C. Shi, R. H. Fan, K. L. Yan, K. Sun, M. Zhang, C. G. Wang, X. F. Liu and X. H. Zhang, Preparation of iron networks hosted in porous alumina with tunable negative permittivity and permeability, *Adv. Funct. Mater.*, 2013, **23**, 4123–4132.

12 S. H. Liu and J. W. Zhai, Improving the Dielectric Constant and Energy Density of Poly(vinylidene fluoride) Composites Induced by Surface-Modified $SrTiO_3$ Nanofibers by Polyvinylpyrrolidone, *J. Mater. Chem. A*, 2015, **3**, 1511–1517.

13 H. Luo, D. Zhang, C. Jiang, X. Yuan, C. Chen and K. C. Zhou, Improved Dielectric Properties and Energy Storage Density of Poly(vinylidene fluoride-*co*-hexafluoropropylene) Nanocomposite with Hydantoin Epoxy Resin Coated $BaTiO_3$, *ACS Appl. Mater. Interfaces*, 2015, **7**, 8061–8069.

14 P. H. Hu, Y. Shen, Y. H. Guan, X. H. Zhang, Y. H. Lin, Q. M. Zhang and C. W. Nan, Topological-Structure Modulated Polymer Nanocomposites Exhibiting Highly Enhanced Dielectric Strength and Energy Density, *Adv. Funct. Mater.*, 2014, **24**, 3172–3178.

15 B. C. Luo, X. H. Wang, Q. C. Zhao and L. T. Li, Synthesis, characterization and dielectric properties of surface functionalized ferroelectric ceramic/epoxy resin composites with high dielectric permittivity, *Compos. Sci. Technol.*, 2015, **112**, 1–7.

16 S. H. Cho, J. Lee and J. S. Jang, Poly(vinylidene fluoride)/NH_2-Treated Graphene Nanodot/Reduced Graphene Oxide Nanocomposites with Enhanced Dielectric Performance for Ultrahigh Energy Density Capacitor, *ACS Appl. Mater. Interfaces*, 2015, **7**, 9668–9681.

17 B. H. Wang, L. M. Liu, L. Huang, L. Z. Chi, G. Z. Liang, L. Yuan and A. J. Gu, Fabrication and Origin of High-*k* Carbon Nanotube/Epoxy Composites with Low Dielectric Loss Through Layer-by-Layer Casting Technique, *Carbon*, 2015, **85**, 28–37.

18 Z. R. Wang, T. Hu, X. G. Li, G. R. Han and W. J. Weng, Nano Conductive Particle Dispersed Percolative Thin Film Ceramics with High Permittivity and High tenability, *Appl. Phys. Lett.*, 2012, **100**, 132909.

19 T. Hu, W. J. Zhao, N. Ma and P. Y. Du, Percolative Nanoparticle-Ag/$PbZr_{0.52}Ti_{0.48}O_3$ Composite Thin Film with High Dielectric and Ferroelectric Properties, *J. Mater. Sci.: Mater. Electron.*, 2015, **26**, 448–455.

20 L. Wang, Y. Bai, X. Lu, J. Cao and L. Qiao, Ultra-low Percolation Threshold in Ferrite-Metal Cofired Ceramics Brings Both High Permeability and High permittivity, *Sci. Rep.*, 2015, **5**, 7580.

21 Z. C. Shi, F. Mao, J. Wang, R. H. Fan and X. Wang, Percolative silver/alumina composites with radio frequency dielectric resonance induced negative permittivity, *RSC Adv.*, 2015, **5**, 107307–107312.

22 R. M. Mutiso and K. I. Winey, Electrical Properties of Polymer Nanocomposites Containing rod-like Nanofillers, *Prog. Polym. Sci.*, 2015, **40**, 63–84.

23 Y. Feng, W. L. Li, Y. F. Hou, Y. Yu, W. P. Cao, T. D. Zhang and W. D. Fei, Enhanced Dielectric Properties of PVDF-HFP/$BaTiO_3$-Nanowire Composites Induced by Interfacial Polarization and Wire-Shape, *J. Mater. Chem. C*, 2015, **3**, 1250–1260.

24 E. Tkalya, M. Ghislandi, W. Thielemans, P. Schoot, G. With and C. Koning, Cellulose Nanowhiskers Templating in Conductive Polymer Nanocomposites Reduces Electrical Percolation Threshold 5-Fold, *ACS Macro Lett.*, 2013, **2**, 157–163.

25 N. K. Shrivastava, S. Suin, S. Maiti and B. B. Khatua, Ultralow Electrical Percolation Threshold in Poly(styrene-*co*-acrylonitrile)/Carbon Nanotube Nanocomposites, *Ind. Eng. Chem. Res.*, 2013, **52**, 2858–2868.

26 A. Ameli, M. Nofar, C. B. Park, P. Pötschke and G. Rizvi, Polypropylene/Carbon Nanotube Nano/Microcellular Structures with High Dielectric Permittivity, Low Dielectric Loss, and Low Percolation Threshold, *Carbon*, 2014, **71**, 206–217.

27 Y. Yang, H. L. Sun, B. P. Zhu, Z. Y. Wang, J. H. Wei, R. Xiong, J. Shi, Z. Y. Liu and Q. Q. Lei, Enhanced Dielectric Performance of Three Phase Percolative Composites Based on Thermoplastic-Ceramic Composites and Surface

Modified Carbon Nanotube, *Appl. Phys. Lett.*, 2015, **106**, 012902.

28 L. Ren, J. Zhao, S. J. Wang, B. Z. Han and Z. M. Dang, Dielectric and magnetic properties of Fe@Fe_xO_y/epoxy resin nanocomposites as high-performance electromagnetic insulating materials, *Compos. Sci. Technol.*, 2015, **114**, 57–63.

29 P. Thakur, A. Kool, B. Bagchi, N. A. Hoque, S. Das and P. Nandy, *In Situ* Synthesis of $Ni(OH)_2$ Nanobelt Modified Electroactive Poly(vinylidene fluoride) Thin Films: Remarkable Improvement in Dielectric Properties, *Phys. Chem. Chem. Phys.*, 2015, **17**, 13082–13091.

30 M. Tian, Z. Y. Wei, X. Q. Zan, L. Q. Zhang, J. Zhang, Q. Ma, N. Y. Ning and T. Nishi, Thermally expanded graphene nanoplates/polydimethylsiloxane composites with high dielectric constant, low dielectric loss and improved actuated strain, *Compos. Sci. Technol.*, 2014, **99**, 37–44.

31 Z. Wang, M. R. Fang, H. J. Li, Y. F. Wen, C. Wang and Y. P. Pu, Enhanced dielectric properties in poly(vinylidene fluoride) composites by nanosized $Ba(Fe_{0.5}Nb_{0.5})O_3$ powders, *Compos. Sci. Technol.*, 2015, **117**, 410–416.

32 Z. C. Shi, S. G. Chen, R. H. Fan, X. A. Wang, X. Wang, Z. D. Zhang and K. Sun, Ultra Low Percolation Threshold and Significantly Enhanced Permittivity in Porous Metal-Ceramic Composites, *J. Mater. Chem. C*, 2014, **2**, 6752–6757.

33 A. Ameli, S. Wang, Y. Kazemi, C. B. Park and P. Pötschke, A Facile Method to Increase the Charge Storage Capability of Polymer Nanocomposites, *Nano Energy*, 2015, **15**, 54–65.

34 Z. D. Zhang, R. H. Fan, Z. C. Shi, K. L. Yan, Z. J. Zhang, X. L. Wang and S. X. Dou, Microstructure and metal-dielectric transition behaviour in a percolative Al_2O_3–Fe composite *via* selective reduction, *RSC Adv.*, 2013, **3**, 26110–26115.

35 Z. D. Zhang, R. H. Fan, Z. C. Shi, S. B. Pan, K. L. Yan, K. Sun, J. D. Zhang, X. F. Liu, X. L. Wang and S. X. Dou, Tunable negative permittivity behavior and conductor–insulator transition in dual composites prepared by selective reduction reaction, *J. Mater. Chem. C*, 2013, **1**, 79–85.

36 M. Gao, Z. C. Shi, R. H. Fan, L. Qian, Z. D. Zhang and J. Y. Guo, High-Frequency Negative Permittivity from Fe/Al_2O_3 Composites with High Metal Contents, *J. Am. Ceram. Soc.*, 2012, **95**, 67–70.

37 Z. C. Shi, S. G. Chen, K. Sun, X. Wang, R. H. Fan and X. A. Wang, Tunable Radio-Frequency Negative Permittivity in Nickel-Alumina "Natural" Metacomposites, *Appl. Phys. Lett.*, 2014, **104**, 252908.

38 Z. C. Shi, R. H. Fan, X. Wang, Z. D. Zhang, L. Qian, L. Yin and Y. J. Bai, Radio-Frequency Permeability and Permittivity Spectra of Copper/Yttrium Iron Garnet Cermet Prepared at Low Temperatures, *J. Eur. Ceram. Soc.*, 2015, **35**, 1219–1225.

39 W. Zhang, H. G. Xiong, S. K. Wang, M. Li and Y. Z. Gu, Negative Permittivity Behavior of Aligned Carbon Nanotube Films, *Appl. Phys. Lett.*, 2015, **106**, 182905.

40 X. Zhang, X. R. Yan, Q. L. He, H. G. Wei, J. Long, J. Guo, H. B. Gu, J. F. Yu, J. J. Liu, D. W. Ding, L. Y. Sun, S. Y. Wei and Z. H. Guo, Electrically Conductive Polypropylene Nanocomposites with Negative Permittivity at Low Carbon Nanotube Loading Levels, *ACS Appl. Mater. Interfaces*, 2015, **7**, 6125–6138.

41 T. Tsutaoka, T. Kasagi, S. Yamamoto and K. Hatakeyama, Double Negative Electromagnetic Property of Granular Composite Materials in the Microwave Range, *J. Magn. Magn. Mater.*, 2015, **383**, 139–143.

42 B. Qiu, J. Guo, Y. R. Wang, X. Wei, Q. Wang, D. Z. Sun, M. A. Khan, D. P. Young, R. O. Connor, X. H. Huang, X. Zhang, B. L. Weeks, S. Y. Wei and Z. H. Guo, Dielectric Properties and Magnetoresistance Behavior of Polyaniline Coated Carbon Fabrics, *J. Mater. Chem. C*, 2015, **3**, 3989–3998.

43 Z. Chen, L. Y. Xie, X. Y. Huang, S. T. Li and P. K. Jiang, Achieving large dielectric property improvement in polymer/carbon nanotube composites by engineering the nanotube surface *via* atom transfer radical polymerization, *Carbon*, 2015, **95**, 895–903.

44 X. R. Xiao, H. Yang, N. X. Xu, L. Hu and Q. L. Zhang, High performance of P(VDF-HFP)/Ag@TiO_2 hybrid films with enhanced dielectric permittivity and low dielectric loss, *RSC Adv.*, 2015, **5**, 79342–79347.

45 L. Weng, H. X. Li, P. H. Ju, T. Wang and L. Z. Liu, The effects of TiC@AlOOH core–shell nanoparticles on the dielectric properties of PVDF based nanocomposites, *RSC Adv.*, 2016, **6**, 25015–25022.

46 *Agilent Impedance Measurement Handbook 5950-3000*, Agilent Technologies, USA, 2009.